Journal of Coastal Research	26	4	622–634	West Palm Beach, Florida	July 2010

Distal Run-up Records of Latest Holocene Paleotsunami Inundation in Alluvial Flood Plains: Neskowin and Beaver Creek, Oregon, Central Cascadia Margin, West Coast U.S.A.

Curt D. Peterson†, Kenneth M. Cruikshank†, Robert B. Schlichting‡, and Scott Braunsten†

†Geology Department
Portland State University
Portland, Oregon 97207-0751, U.S.A.
petersonc@pdx.edu

‡Cleaveland High School
Portland, Oregon 97202, U.S.A.

ABSTRACT

PETERSON, C.D; CRUIKSHANK, K.M.; SCHLICHTING, R.B., and BRAUNSTEN, S., 2010. Distal run-up records of latest Holocene paleotsunami inundation in alluvial flood plains: Neskowin and Beaver Creek, Oregon, Central Cascadia Margin, West Coast U.S.A. *Journal of Coastal Research,* 26(4), 622–634. West Palm Beach (Florida), ISSN 0749-0208.

Paleotsunami records in two localities of the central Cascadia margin, Neskowin and Beaver (West Coast, U.S.A., Northeast Pacific Ocean coast), are extended landward to distal flood plain settings. Three paleotsunami sand sheets are correlated to Cascadia subduction zone earthquakes, between 0.3 and ~1.3 ka in age. One older paleotsunami layer (2960–3220 cal YBP) is apparent in some deeper core sites from the Beaver Creek locality. Marine sand (22%–100%) and marine diatoms (40%–100%) from the distal sand sheets distinguish the catastrophic marine inundations from creek floods. The greatest inundations are correlated to two Cascadia paleotsunami events, #3 at ~1.3 ka and an older event between ~2.6 and ~3.2 ka, based on radiocarbon dating and great earthquake sequence. The best-preserved records are from paleotsunami #3, which reached 4.1 km in overland inundation up the North Beaver flood plain (3 m elevation North American Vertical Datum). At the Neskowin locality, a sand sheet from the #3 paleotsunami was traced to 8.3 m elevation in the Hawk flood plain. Adjusting for paleosea level at 1.3 ka, we estimate that the #3 paleotsunami run-up height reached 9 m at a landward distance of 1.0 km in Neskowin. The paleotsunami sand sheets in Neskowin and Beaver represent the maximum recorded distal run-up for Cascadia paleotsunami reported to date. The potential for preservation of marine surge deposits in alluvial flood plains should greatly extend the geologic record of prehistoric inundations in other susceptible coastlines.

ADDITIONAL INDEX WORDS: *Distal deposits, debris layers, heavy minerals, diatoms, radiocarbon dating, stratigraphic correlation.*

INTRODUCTION

Two small flood-plain localities, Neskowin and Beaver, are examined for distal run-up records preserved from latest Holocene paleotsunami in the central Cascadia margin (Figure 1). The 1000-km long Cascadia subduction zone has not ruptured in historic time, but it has a long history of megathrust earthquakes (Atwater, 1987), with recurrence intervals of about 500 years (Atwater *et al.,* 2004; Darienzo and Peterson, 1990). Paleotsunami sand layers from the last rupture estimated to be ~9 Moment Magnitude Scale (Mw) at 1700 AD (Satake *et al.,* 1996) are reported from the full length of the subduction zone (Atwater *et al.,* 1995). Paleotsunami sand layers are known from peat and mud hosting deposits in estuary marshes (Clague and Bobrowsky, 1994; Darienzo, Peterson, and Clough, 1994), back-barrier wetlands (Abramson, 1998; Schlichting and Peterson, 2006) and barrage ponds (Kelsey *et al.,* 2005), but not from higher-elevation settings that can yield maximum-recorded run-ups. The Neskowin and Beaver localities contain alluvial flood plain settings that extend well above or beyond their proximal back-barrier wetlands. Both localities were known to have recorded multiple events of overland paleotsunami inundation in their back-barrier ponds and wetlands (Alhadeff *et al.,* 1988; Boynay *et al.,* 1994; Schlichting, 2000). The preservation of multiple sand sheets together with contrasting elevations of flood plains in these paired localities make them ideal candidates for tracing paleotsunami surge records further landward in alluvial flood plains. Successful recognition of marine surge deposits in flood plain settings should motivate new searches for prehistoric run-up evidence in other coastlines (Dawson and Shi, 2000).

The Neskowin and Beaver flood plains differ in their protection by seaward barriers and in their landward elevation gradients. The two localities are similar in (1) relatively straight coastlines, (2) uniform offshore gradients, and (3) abundant sand in beach and inner-shelf deposits (Peterson *et al.,* 1994). The littoral and river sands from the study area differ in both grain rounding and mineralogy (Clemens and Komar, 1988; Peterson, Scheidegger, and Komar, 1982), permitting the discrimination of river and marine surge flooding.

DOI: 10.2112/08-1147.1 received 23 October 2008; accepted in revision 29 January 2009.

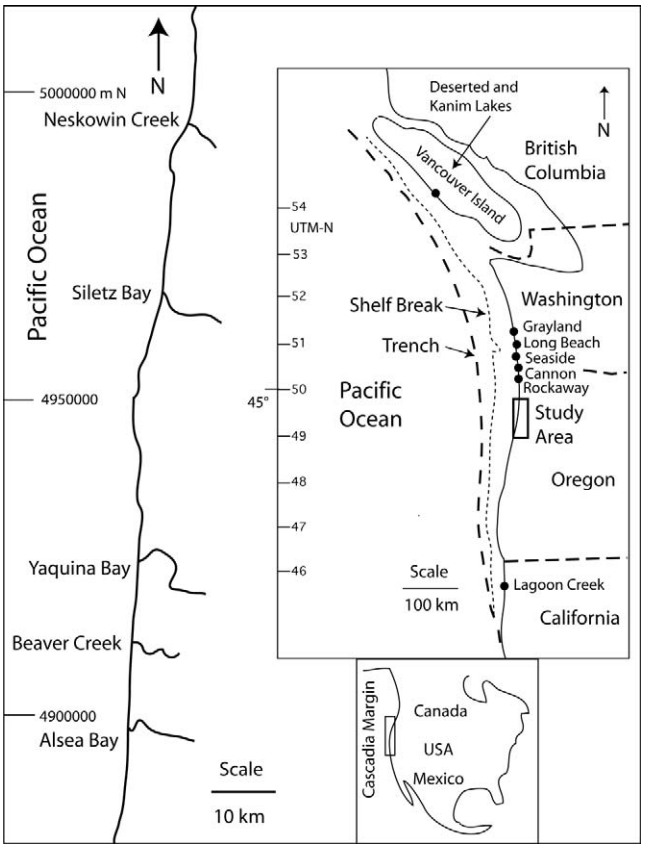

Figure 1. Location maps of the Casadia subduction zone with trench (~2000 m depth), shelf break (~250 m depth), and localities of reported paleotsunami overland inundation (0.5–1.0 km distance) in the central Cascadia margin including Grayland and Long Beach, Washington, and Seaside, Cannon Beach, and Rockaway, Oregon (Peterson, Cruikshank, and Schlichting, 2008; Schlichting and Peterson, 2006). Overland paleotsunami inundation is also reported for Deserted and Kanim lakes in Vancouver Island, British Columbia (Hutchinson, Clague, and Mathewes, 1997; Hutchinson *et al.,* 2000) and for Lagoon Creek in northernmost California (Abramson, 1998; Garrison-Laney, 1998). Inset of the study area shows localities of paleotsunami inundation in three small estuaries, Siletz Bay, Yaquina Bay, and Alsea Bay, and in two alluvial floodplain localities, Neskowin and Beaver Creek. Position coordinates are in UTM (m) northing and reference latitude and longitude (°).

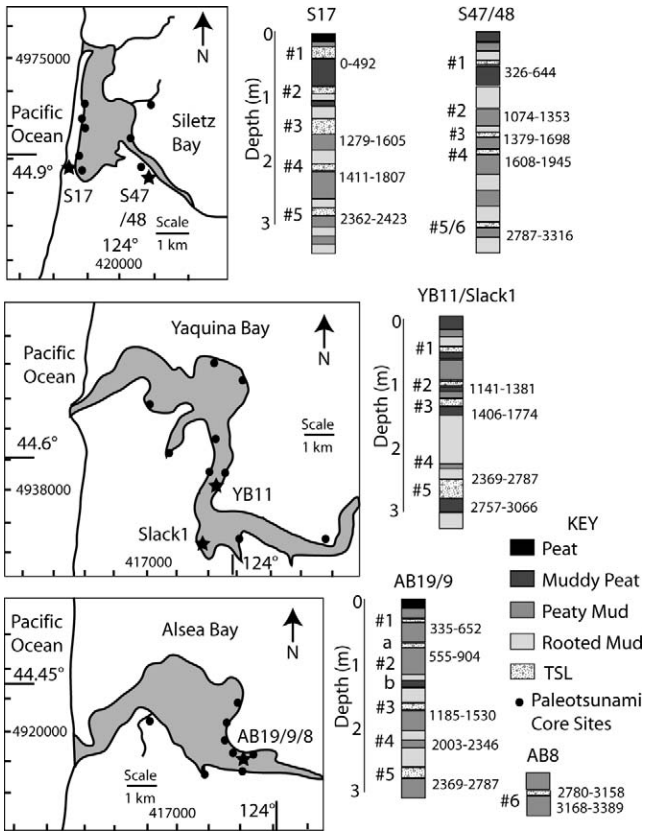

Figure 2. Maps of Siletz, Yaquina, and Alsea bays showing reported paleotsunami sites (solid circles) and dated core sequences (solid stars) of paleosubsidence and paleotsunami sand layers (TSL). Depth is in meters (m) subsurface. Tsunami sand layers overlie peaty marsh surfaces. Abrupt upcore decreases in peat : mud ratio indicate coseismic subsidence of the tidal marshes produced by ruptures of the Cascadia megathrust (events #1–6). Bulk peat dates are shown for corresponding intervals in calibrated radiocarbon years (2-σ uncertainty). See Table 1 for event ages and detailed radiocarbon data. Core log data from Darienzo (1991), Peterson and Darienzo (1997), Peterson and Priest (1995), and Peterson *et al.* (1996). Position coordinates are in UTM (m) and reference latitude and longitude (°).

The paleotsunami run-up records presented here can be used to evaluate tsunami evacuation strategies for the central Cascadia margin. These run-up records can also be compared with overland run-up events dated in representative sites from central, northernmost, and southernmost Cascadia margin (Abramson, 1998; Hutchinson, Clague, and Mathewes, 1997; Hutchinson *et al.,* 2000; Schlichting and Peterson, 2006). Such marginwide correlations of overland run-up events should provide constraints on regional paleotsunami hazard in the Cascadia subduction zone (Figure 1). In a broader context, the methods shown here provide a framework for extending the geologic records of tsunami run-up (Shiki *et al.,* 2008) to their maximum preserved landward extent in alluvial settings.

BACKGROUND

The recognition and dating of paleotsunami deposits in alluvial settings are made difficult by channel migrations, river flood deposits, descending roots, bioturbation, and seasonal oxidation (see Results below). Paleotsunami investigations in such settings should start with a well-constrained record of paleotsunami inundations in the study area.

Paleotsunami inundation of small estuaries in the central Oregon coast, such as Siletz, Yaquina, and Alsea bays (Figure 1), have been established (Darienzo, 1991; Peterson and Priest, 1995; Peterson *et al.,* 1996). Catastrophic inundation deposits in the estuary wetlands are identified by anomalous sand or muddy sand layers (1–30 cm thick), which are hosted in peaty mud (Figure 2; Table 1). Heavy-mineral analyses of suspected paleotsunami sand layers are used to confirm their origins from marine surges in the small estuaries (Figure 2;

Table 1. *Dated events of paleosubsidence horizons that underlie paleotsunami sand layers in small tidal basins of central Oregon.*

Bay/Site Record	Event (age ka)	Depth (m)	adjC14 adjRCYBP	Cal RC 1-σ calRCYBP	Cal RC 2-σ calRCYBP	Lab Beta #
Siletz						
SB17						
Sub/TSL	Y, 1, 0.3	0.5	270 ± 60	153–437	0–492	B42089
TSL	*, 2 ~0.8	0.7	—			
Sub	W, 3 ~1.1	1.1	—			
Sub/TSL	U, 4 ~1.3	1.5	1510 ± 90	1318–1515	1279–1605	B42001
Sub/TSL	S, 5 ~1.7	2.1	1690 ± 70	1528–1695	1411–1807	B42091
Sub/TSL	N, 6 ~2.6	2.7	2550 ± 80	2491–2753	2362–2423	B42002
SB47/48						
Sub/TSL	Y, 1, 0.3	0.5	480 ± 60	480–620	326–644	B42085
TSL	*, 2 ~0.8	0.7	—			
Sub	W, 3 ~1.1	1.1	1330 ± 70	1178–1305	1074–1353	B43126
Sub/TSL	U, 4 ~1.3	1.5	1630 ± 70	1415–1600	1379–1698	B43125
Sub/TSL	S, 5 ~1.7	2.0	1850 ± 70	1712–1869	1608–1945	B42086
Sub/TSL	N, 6 ~2.6	3.0	2880 ± 90	2880–3156	2787–3316	B42087
Yaquina						
YB11/S1						
Sub/TSL	Y, 1, 0.3	0.5	—			
Sub/TSL	*, 2, ~0.8	0.8	—			
Sub	W, 3 ~1.1	1.1	1350 ± 60	1182–1315	1141–1381	B42092
Sub/TSL	U, 4 ~1.3	1.7	1680 ± 70	1522–1695	1406–1774	B42093
Sub	S, 5 ~1.7	2.5?	—			
Sub/TSL	N, 6 ~2.6	2.7	2570 ± 60	2505–2757	2369–2787	B42094
—	—	3.1	2780 ± 70	2791–2953	2757–3066	B42095
Alsea						
AB9/19						
Sub/TSL	Y, 1, 0.3	0.4	500 ± 60	499–624	335–652	B39181
TSL	*, 2 ~0.8	1.1	760 ± 80	574–774	555–904	B27184
Sub	W, 3 ~1.1	1.3	—			
Sub/TSL	U, 4 ~1.3	1.7	1450 ± 80	1287–1413	1185–1530	B26791
		2.4	2200 ± 80	2140–2325	2003–2346	B27185
Sub/TSL	N, 6 ~2.6	3.2	2570 ± 60	2505–2757	2369–2787	B26792

Event subsidence (Sub) and/or tsunami sand layer (TSL) in reported core sites from Siletz Bay (SB) (Peterson *et al.,* 1996); Yaquina Bay (YB) (Darienzo, 1991; Peterson and Priest, 1995); and Alsea Bay (AB) (Peterson and Darienzo, 1997). Rupture events are shown by letter code (Y, W, U, S, N) (Atwater *et al.,* 2004), central Cascadia paleotsunami number (1–6) (Peterson *et al.,* 2008); and corresponding date (~ ka) (Atwater *et al.,* 2004). Subsidence horizons are inconsistently recorded between core sites in these central Oregon bays, which are located near a zero-isobase (Peterson, Doyle, and Barnett, 2000). Paleotsunami event #2 (estimated age ~0.8 ka) is of uncertain origin in the central Cascadia margin because it generally lacks an associated subsidence event. It is referred to as an orphan tsunami for the Cascadia margin (Clague and Brobowsky, 1994; Schlichting, 2000). The subsidence horizons in the small bays were dated by standard radiocarbon technique prior to AMS dating practices. Bulk peaty intervals (5–10 cm thick) are assumed to generally predate the radiocarbon ages of the correlative Cascadia ruptures and associated tsunami in the central Cascadia margin. The adjusted radiocarbon ages (adjC14) have been calibrated with CALIB 5.0.2 (Reimer *et al.,* 2004) for 1 σ and 2 σ uncertainties. Beta Analytic Inc. (Lab no.) performed the radiocarbon dating of submitted peaty intervals in the three tidal basins.

* Indicates 'orphan tsunami' for the central Cascadia margin. Its origin is unknown.

Peterson and Darienzo, 1997). The paleotsunami layers directly overlie abruptly subsided marsh surfaces, demonstrating coseismic-rupture origins of the catastrophic inundations. The tsunami sand layers typically display fining-upward sequences of sand and silt. There are no equivalent flooding records in these bays since the last Cascadia rupture at 1700 AD. Storm surge, tidal inlet migration, and/or other aseismic autocylic processes (Shennan *et al.,* 1998) do not account for the associated abrupt subsidence and catastrophic marine inundations in these small estuaries.

Stratigraphic correlations of the paleotsunami events in the small bays (Figure 2) are based on their association with minor coseismic subsidence (~0.5 m) in this part of the Cascadia subduction zone (Darienzo, 1991; Peterson, Doyle, and Barnett, 2000). As many as six nearfield paleotsunami inundations are recorded during the last ~3 ka in the three small bays. Five of the paleotsunami inundations (events #1–5) are correlated to central Cascadia ruptures by radiocarbon dating of the abruptly subsided peaty horizons as shown in Table 1.

An orphan sand layer, lacking a coseismic subsidence horizon, is observed between subsidence events #1 and #2 in some northern Cascadia localities (Clague and Brobowsky, 1994; Peterson *et al.,* 2008). The orphan tsunami layer is dated 555–904 cal YBP at ~0.7 m depth in the Alsea Bay core site AB19/9. The origin of this sand layer is not known, but it might represent a partial rupture of the Cascadia margin (Schlichting, 2000). For this compilation we identify the couplet of paleotsunami layers below the 1700 AD tsunami deposit as event #2 layers a and b, where a refers to the orphan paleotsunami sand layer (Figure 2). Where only a single layer is recorded, with or without a subsidence horizon, we identify it as event #2. The well-recorded paleotsunami inundations are directly correlated to Cascadia megathrust ruptures at

0.3, ~1.1, ~1.3, ~1.7, and ~2.6 ka by number and dated sequence in the central Oregon bays (Table 1).

Particularly robust tsunami inundations of the small bays in central Oregon (Figure 2) are shown by (1) thickness of paleotsunami sand layers, (2) continuity of sand layers in the lower bay reaches, and (3) landward extent of the sand layers in the upper reaches of the small estuaries. The three greatest inundations are associated with central Cascadia events #1 (0.3 ka), #3 (~1.3 ka), and #5 (~2.6 ka). Paleotsunami inundation of the shallow bays reached at least 5 km in Siletz Bay, 11 km in Yaquina Bay, and 7 km in Alsea Bay (Figure 2). The estuaries link rupture subsidence to nearfield tsunami excitation. They do not provide a direct measure of the paleotsunami run-up magnitude. That is due, in part, to poorly constrained tidal levels in the bays during prehistoric inundations.

Overland paleotsunami inundations in back-barrier wetlands of the central Cascadia margin are reported from Grayland, and Long Beach, Washington, and Seaside, Rockaway, and Neskowin, Oregon (Figure 1) (Fiedorowicz, 1997; Schlichting, 2000). Overland inundations in these central Cascadia localities are linked to Cascadia paleotsunami, as based on (1) landward thinning deposits, (2) marine surge tracers, and (3) approximate event recurrence intervals (Schlichting and Peterson, 2006). Radiocarbon dating of the overland tsunami inundations in the Cascadia margin has been problematic. The supratidal wetlands do not record coseismic subsidence that is associated with nearfield tsunami excitation. The violent remobilization of preexisting peat, forest litter, and soils by overland paleotsunami surges can yield reversed dates downcore (Abramson, 1998; Clague and Bobrowsky, 1994). Regional correlation of the overland tsunami inundations is partly dependent on proxy records from nearby tidal basins (Figure 2; Table 1).

The back-barrier settings do provide minimum run-up estimates (6–8 m) based on minimum surge heights that are necessary to overtop barrier ridges (Peterson *et al.,* 2006). Such minimum estimates are further limited by (1) the uncertainty of barrier sand ridge heights at the time of overtopping and (2) narrow landward widths of the back-barrier wetlands (0.5–1.5 km landward distance). Soil peds found in paleotsuanmi deposits from the wetland back edges indicate hill-slope backwash in Grayland, Seaside, and Rockaway (Figure 1) (Darienzo *et al.,* 1993; Fiedorowicz, 1998; Schlicting, 2000). Maximum recorded inundation in these narrow wetlands underestimates the furthest landward run-ups. The first attempt to extend the Cascadia paleotsunami records landward of the back-barrier wetlands was conducted in Cannon Beach, Oregon (Peterson *et al.,* 2008). One back-barrier sand sheet (1276–1411 cal YBP) was traced an additional 1000 m landward in alluvial flood plain deposits that reach 3–4 m elevation above the back-barrier wetlands. That approach is reapplied in this study of the two contrasting flood plain settings formed at Neskowin and Beaver.

STUDY AREA LOCALITIES

The Neskowin and Beaver localities (Figure 1) differ in the extent of their seaward barrier ridges and landward flood plains. The small creek mouths are silled by summer beach sand accretion, but they discharge directly to the ocean during peak winter floods (mean annual discharge ~1.5 $m^3 s^{-1}$; U.S. Geological Survey Water Resources, 2007). The narrow Neskowin flood plain (~0.5 km in landward width) is partially protected by abandoned foredune ridges (Figure 3). The ridges increase in number (1–3) and height (5–8 m elevation) from north to south. Elevations presented here are relative to the 0-m North American Vertical Datum NAVD88, which is about 1 m below mean tidal level. The mean high water–mean low water tidal range is ±1.5 m in the study area. The Neskowin back-barrier wetlands are supratidal (3–4 m elevation), having filled in the back-barrier lagoon by about 1.5 ka (Schlichting, 2000). The Neskowin wetlands locally extend upslope to 5–15 m elevation in a small upland flood plain of Hawk Creek, at distances of 1–1.5 km from the present ocean shoreline.

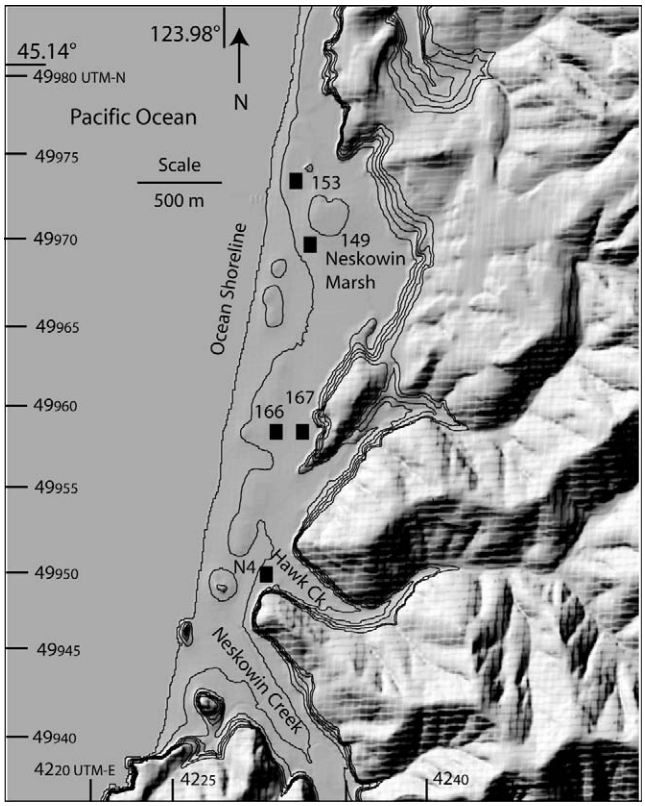

Figure 3. Shaded relief map of the Neskowin flood plain locality in central Oregon, showing selected back-barrier core sites with paleotsunami deposits (solid squares). The back-barrier wetlands of the Neskowin marsh extend upslope to 10–15 m elevation in the small upland flood plain of Hawk Creek. Topographic contours (lines) are shown for 0, 5, 10, 15, and 20 m elevations, approximated by a digital elevation model (DEM) provided via the Seamless Map Data Web site (U.S. Geological Survey, 2008). Position coordinates are in UTM (m) and reference latitude and longitude (°).

The Beaver flood plain is generally unprotected by barrier foredunes at its narrow mouth (Figure 4). The lowland flood plain (2–4 m elevation) extends 4–5 km landward along Bea-

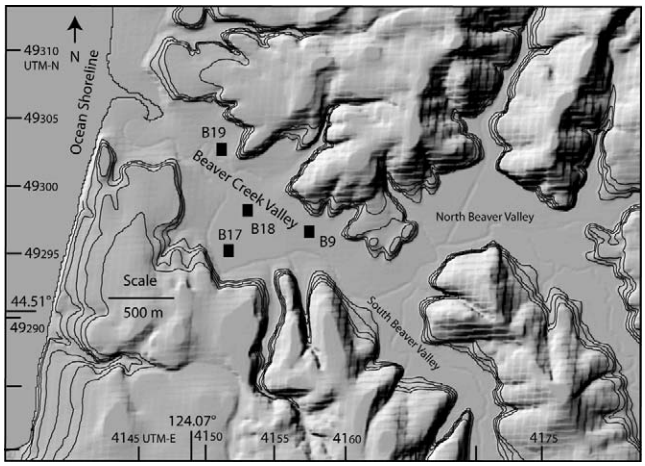

Figure 4. Shaded relief map of the Beaver Creek flood plain locality in central Oregon showing selected back barrier cove sites with paleotsunami deposits (solid squares). The creek mouth wetlands extend about 5 km up-creek into the North and South Beaver Creek valleys at 2–4 m elevaion. Topographic contours (lines) are shown for 0, 5, 10, 15, and 20 m elevations, approximated by a DEM provided via the Seamless Map Data Web site (U.S. Geological Survey, 2008). Position coordinates are in UTM (m) and reference latitude and longitude (°).

ver Creek from the ocean shoreline. The Beaver flood plain is broad (0.5 km in width) relative to the very small Beaver Creek. The supratidal wetlands in the lower Beaver flood plain (2 m elevation) are flooded year round, forming a pallustrine peaty bog. Upstream of the Beaver Creek confluence, the flood plain (3 m elevation) is only flooded during wet winter periods.

FIELD METHODS

Core sampling was performed by gouge core (2.5 cm diameter) and ram core (7.5 cm diameter) to ~2.0 m depth in the Neskowin and Beaver flood plains. The larger diameter cores yield better sedimentary sections but suffer from shallow refusal in dried and compacted flood plain soils. Tributary cut banks were modified in early historic time, and deep trenches are limited by shallow groundwater levels.

Core sites were generally laid out in across-valley transects, with a minimum of 3–5 cores examined from each core site (~10 m² area). Up to 10 cores were taken at some sites. The nested sampling strategy was necessary to identify intact tsunami sand layers (TSL) and sandy organic-debris layers (TDL) in substantially bioturbated soils. About 50 cores each were examined in the Hawk Creek upland flood plain at Neskowin and in the North Beaver Creek valley. Representative cores were subsampled for radiocarbon, sand mineralogy, and diatom analyses. Core positions are established by Wide Area Augmentation System Global Position System (waasGPS) (±10 m) (Cruikshank and Peterson, 2008). Core site elevations are established by total station surveying to registered benchmarks or by GPS postprocessing differential correction (~0.1 m elevation control).

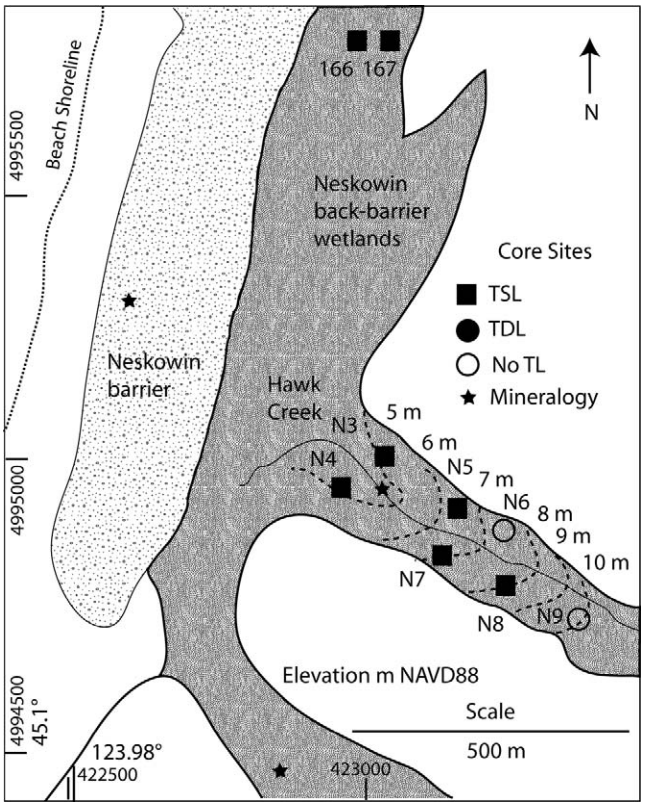

Figure 5. Map of core sites from the Neskowin upland flood plain developed on either side of the very small Hawk Creek tributary. Elevation contours (dashed lines) are at 1-m intervals (5 to 10 m North American Vertical Datum NAVD88). Core sites are shown that contain a target paleotsunami sand layer (TSL solid black square), paleotsunami debris layer (TDL solid black circle), or no apparent tsunami deposit (open circle). Beach and river sand samples were collected from the Neskowin barrier and Hawk Creek tributaries (solid stars). Position coordinates are in UTM (m) and reference latitude and longitude (°).

RESULTS

Neskowin Inundation Records

Paleotsunami inundations in the back-barrier wetlands of Neskowin (Figure 3) are mapped from anomalous sand sheets (up to 40 cm in thickness) that thin with increasing distance landward (Schlichting, 2000). Representative core sites from the Neskowin back-barrier wetlands demonstrate barrier overtopping and inundation from several paleotsunami events (Figure 5). Suspected paleotsunami layers in the flood plain are identified in the field by quartz-rich "beach" sand (Figure 6) but are sampled for microscopic analysis of heavy minerals and diatoms to confirm marine surge origins.

The back-barrier core sites that are most proximal to the Neskowin barrier demonstrate 3–4 distinct sand layers hosted in peat or peaty mud deposits (Figure 7). A peat layer in direct contact with the deepest tsunami sand layer in site 153 is dated at 920–1320 cal YBP (Table 2). The mapped sand sheets in the Neskowin back-barrier wetlands are correlated to the last three Cascadia events #1–3 (Table 1). The second

Figure 6. Photograph of two sand types including: (1) target paleotsunami event #3 deposit in site N3 (light: quartz-rich) in photo left, and (2) creek bank deposit in Hawk Creek (dark: lithic-rich) in photo right. Target paleotsunami sand grains are generally well sorted, ranging from ~100–300 μm in diameter. Hawk Creek sediments range from silt in the flood plain to sand and gravel in the creek bed. Mesh screen size is 50 μm in the minisieve (2.5 cm diameer) displaying the two different sand lithologies.

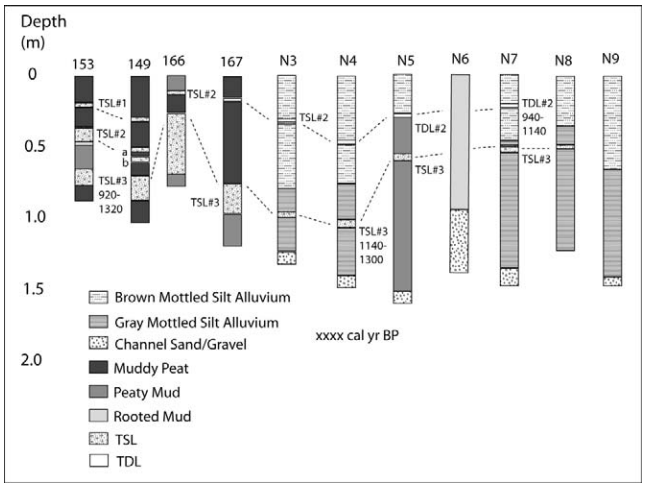

Figure 7. Core logs from the Neskowin lowland flood plain (153, 166, 167) and Hawk Creek upland flood plain (N3–N9). Two out of three to four paleotsunami sand sheets are traced from back-barrier wetlands to the Hawk Creek flood plain. The upper sand sheet (event #2) pinches out to a tsunami debris layer, dated 940–1140 cal YBP at site N7. The lower sand sheet, dated at 1140–1300 cal YBP at site N4, is tracked to N8. See Figure 5 for core site locations and elevations, Table 2 for detailed radiocarbon data, and Table 1 for correlative Cascadia paleotsunami events. Tsunami sand layers (TSL) and tsunami debris layers (TDL) are very inconsistently preserved in bioturbated flood plain deposits.

paleotsunami deposit (#2) in site 149 shows a couplet of sand layers including layers a and b, which are separated by a thin peaty layer. Because of uncertainty about the origins of the couplet (Schlichting, 2000), we refer to it as event #2 (Figure 2, Table 1). The event #3 sand layer in Neskowin is substantially thicker than the preceding sand layers in most cores sites (Figure 7).

A small upland flood plain rises from the Neskowin back-barrier wetlands (2–4 m elevation) to more than 10 m elevation, at a distance of ~1.25 km from the ocean shoreline (Figure 5). The narrow flood plain (100–200 m wide) is developed on either side of a very-small tributary, Hawk Creek (~3 m width bank-to-bank). Coring in the upland flood plain soils reveals paleotsunami deposits in sites that reach elevations of 7–8 m.

Core logs from Neskowin (Figure 7) demonstrate the landward thinning of paleotsunami sand layers from back-barrier sites 166 and 167 (15–40 cm thick) to upland flood plain sites N7 and N8 (1–2 cm thick). The abrupt thinning occurs over a distance of only 500 m from the Neskowin barrier, but with an elevation gain of 5–6 m from the back-barrier wetlands to the upper flood plain soils (Figure 5).

Two paleotsunami layers are inconsistently preserved in sites from the Hawk Creek flood plain. The lower sand layer reaches about 6 cm in thickness at about 1 m depth in site N4 (Figure 7). It is dated from embedded leaf fragments at 1140–1300 cal YBP (Table 2). The sand sheet is traced at shallower depths (~0.5 m depth) to sites N5, N7, and N8.

Table 2. *Neskowin and Beaver radiocarbon dates.*

Locality Core Site	Depth (m)	Event #	adjC14 adjRCYBP	Cal RC 1-σ calRCYBP	Cal RC 2-σ calRCYBP	Lab Beta #
Neskowin						
153	0.75	3–4	1180 ± 100		920–1320	120440
N4	1.04	4	1300 ± 50	1180–1290	1140–1300	244553
N7	0.22	3	1120 ± 40	970–1060	940–1140	244554
Beaver						
B2	0.52	1	410 ± 40	470–510	320–520	247807
B2	1.68	4	1690 ± 40	1540–1680	1520–1700	228596
B20	2.66	6–7?	2930 ± 40	3000–3160	2960–3220	247808

Radiocarbon dated wood fragments (twigs and bark) from target paleotsunami layers (core site) and depth (m).
Radiocarbon dates include adjusted (adj) radiocarbon years before present, Calibrated radiocarbon (at 1 and 2 sigma uncertainty), and the Laboratory sample number (Beta Analytic Inc.).
Woody fragments were used for dating some target layers rather than embedded leaves or rhizomes. The latter are hard to differentiate from descending roots, which can introduce young carbon into the flood plain deposits. Woody fragments can predate the inundation event, particularly where catastrophic inundation remobilized preexisting soils in the heavily vegetated flood plains.

Figure 8. Photograph of bioturbated paleotsunami sand layer (event #3) at site N3 in Neskowin upland flood plain. Grains of quartz-rich beach sand (light) are dispersed in gray silt of allulvial flood plain deposits (dark) by postdepositional bioturbation. Photo is scaled (1-cm intervals) in the field by tape measure.

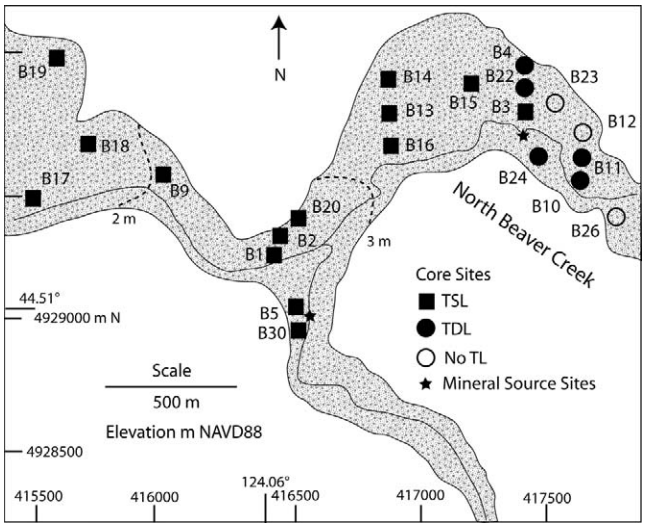

Figure 9. Map of core sites from upper Beaver valley flood plains. Contours (dashed lines) are at 1-m intervals (2 to 3 m elevation North American Vertical Datum). Core sites are shown that contain target paleotsunami sand layers (TSL solid black square), or target debris layer (TDL solid black circle) or no apparent paleotsunami deposit (open circle). Position coordinates are in UTM (m) and reference latitude and longitude (°).

Bioturbation has dispersed the quartz-rich "beach" sand in the paleotsunami sand layers within the hosting flood plain silts (Figure 8).

The upper paleotsunami sand layer (~0.25 m depth) in the Hawk Creek flood plain sites consists of quartz-rich "beach" sand disseminated in detrital organics (Figure 7). Such detrital organics, silt, and disseminated sand grains are swept inland with overland tsunami inundation. We refer to the laminae of rare disseminated "beach" sand in detrital organics and silt as tsunami debris layers (Peterson *et al.,* 2008). The tsunami debris layer, at a depth of 22 cm, in site N7, is dated by detrital organic fragments, yielding an age of 940–1140 cal YBP (Table 2). Based on the sequence of sand layers in the Neskowin back-barrier wetlands and the radiocarbon dates of the two sand layers in the Hawk Creek flood plain (Table 2), we identify the Hawk Creek inundations as Cascadia paleotsunami events #2 and #3.

A pinch out of the #2 paleotsuami deposit between sites N7 and N8 limits the recorded run-up of this event to ~7 m elevation at a distance of ~1 km from the beach. The #3 paleotsunami sand layer is present at site N8 but could not be traced further landward because of excessive bioturbation in the soils of the Hawk Creek flood plain. The #3 inundation event reached at least 8 m elevation at a distance of 1.0 km from the beach at Neskowin.

Beaver Creek Inundation Records

Shallow cores (1–2 m depth) of peat or peaty mud from back-barrier wetlands in the lower Beaver Creek valley (Figure 4) host 2–3 layers of beach sand, paleotsunami deposits (10–30 cm thick) that thin with increasing distance landward (Alhadeff *et al.,* 1998). At distances of 1.0–1.5 km from the beach, the two uppermost sand sheets thin to sand laminae, and then to sandy debris layers at sites B17 and B18 (Figure 9). A deeper sand sheet (1.3–1.8 m depth) retains a thickness of 5–10 cm at a distance of ~1.5 km from the ocean shoreline (Figure 10a). The widespread distribution of peaty mud in core sites across the Beaver alluvial plain demonstrates a filling of the submerged valley to subaerial flood plain elevations prior to the period of tsunami layer deposition. Overland catastrophic inundation extended across the full width

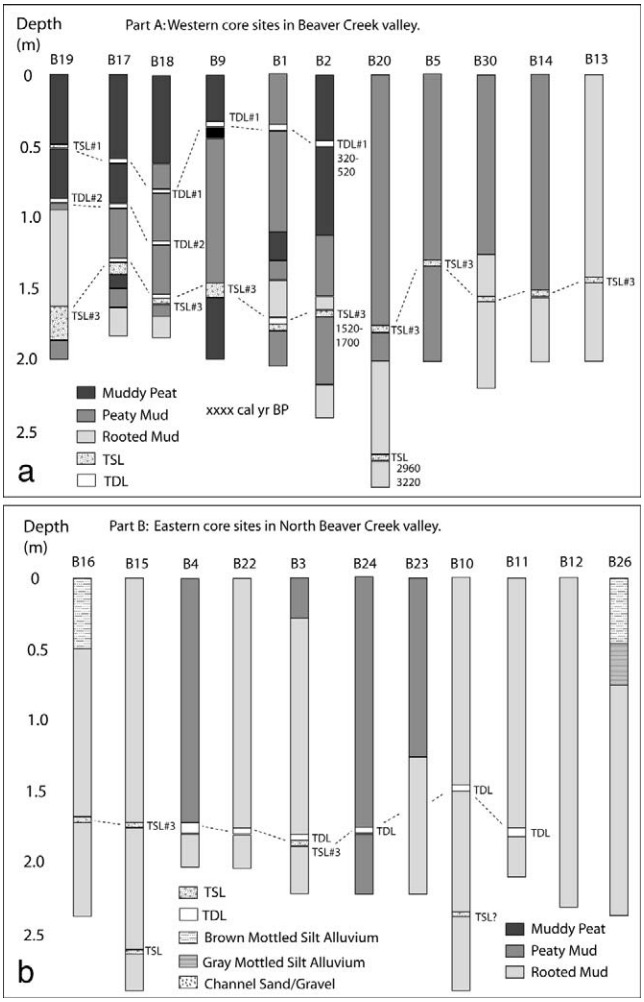

Figure 10. (a) Core logs from west upper North Beaver valley and (b) from east upper North Beaver valley. A shallow tsunami debris layer (event #1) is traced to site B2 where it is dated 320–520 cal YBP. A prominent paleotsunami sand sheet (event #3) is consistently recorded at 1.3 to 1.8 m subsurface depth from sites B19 to B15 in the Beaver flood plain. The sand sheet is dated 1520–1700 cal YBP at site B2. Core sites B20, B15, and possibly B10 contain an older sand sheet (dated 2960–3220 cal YBP) at depths of ~2.5 to 2.7 m. The deeper target layer at ~2.5 m depth (event #5–7?) is poorly preserved. It was not recognized until late in the study, so it was not reached in most core sites (taken to ~2 m depth).

of the Beaver valley, being little influenced by the narrow Beaver Creek.

Core logs from representative sites in the upper Beaver valley (Figures 10a and b) document the landward extent of the deeper paleotsunami sand sheet(s). The sand sheet at 1.3–1.8 m depth is consistently evident in the western core sites from B19 to B15, but pinches out to discontinuous debris layers in the eastern core sites B4, B22, B24, B10, and B11 (Figure 10b).

Three paleotsunami layers are recorded at the grouped sites B1, B2, and B20 at a distance of about 2 km from the ocean shoreline. A shallow debris layer is rarely preserved at ~0.5 m depth at B1 and B2. It is dated from a wood fragment in site B2 at 320–520 cal YBP (Table 2). A widely developed sand layer occurs at ~1.3–1.7 m depth from B2 to B3. Degraded organics embedded in the 1.7 m depth sand layer in site B2 yield an age of 1520–1700. A poorly sampled sand layer occurs in some of the deepest cores sites of the North Beaver Valley. This deepest sand sheet at ~2.66 cm depth in core site B20 is dated to 2960–3220 by large wood fragments in the sand layer. Wood fragments were used to avoid "young carbon" contamination by descending rootlets in the peaty flood-plain deposits. The wood fragments predate the inundation event.

Based on the sequence of three sand layers in the Beaver back-barrier wetlands, and radiocarbon dates corresponding to the first and third layers at site B2, the three upper sand sheets are correlated to Cascadia paleotsunami events #1–3 (Table 1). The deepest recorded sand sheet at ~2.7 m depth in site B20 could correlate to any one of three rupture events (#5–7) that occurred between ~2.6 and ~3.2 ka.

Sand Grain Size

Grain size analyses were performed on sand size grains (62–750 μm diameter) in the bulk light-mineral fraction from paleotsunami deposits and from end-member beach and creek samples. Mean and standard deviation values of sand size are derived from intermediate diameters (D_i) of 50 grains measured per sample under 250× with an ocular micrometer. Results from the grain-size analyses are summarized in Table 3.

The mean grain sizes of the tsunami sand layer #3 in the Neskowin Hawk Creek sites N4 and N7 are 185 and 174 μm, respectively (Table 3). At this locality there is relatively little variation in grain size between the close-spaced core sites (300 m total distance) that differ by 3–4 m in elevation. By comparison, mean grain size of the sand layer #3 does vary substantially over long distances in the low-gradient Beaver valley. The mean grain size decreases from ~220 μm at site B19 to 162 μm at site B3 (Figure 11) over a separation distance of 3 km.

The distal end of the #3 sand sheet in the North Beaver Valley pinch outs out to tsunami debris layers, containing distinctive organic detritus with disseminated "quartz-rich" grains (Figure 12). The mean size of sand grains rafted in with the organics decreases somewhat in site B22 debris layer (mean size ~136 μm), relative to the nearby terminal sand sheet sample at site B3 (mean size 162 μm) (Table 3).

Marine Surge Tracers

Two marine tracers, including heavy minerals and diatoms, are used to formally test the paleotsunami origins of "target" paleotsunami sand layers from the Neskowin and Beaver flood plains. Sand source is based on the relative rounding of first-cycle augite (clinopyroxene) that is locally derived from Coast Range basalts. The monomineralic augite is angular in river sands but is rounded in beach sands, as based on the Powers rounding chart for standardization (Peterson, Schiedegger, and Komar, 1982). One hundred augite grains are counted from the 100–250-μm size range of the

Table 3. *Sand grain size and marine tracers in target paleotsunami deposit layers.*

Core Site	Depth (cm)	Tsunami Event	Mean G.S. (μm)	SD ± 1σ (μm)	Mineral % Marine	Diatom % Marine
Neskowin Beach	—		210	43	100	
Nesk Creek	—		—	—	0	
Hawk Creek	—		296	148	3	
N4	10	Control				19
N4	25	Control				0
N4	47	#3	177	56	76	100
N4	103	#4	185	58	87	52
N4	120	Control				17
N7	50	#4	175	46	85	67
N7	75	Control				14
Beaver Beach	—		228	46	100	
North Creek	—		308	178	0	
South Creek	—				5	
B19	52	#1	188	52	79	
B19	88	#2–3?	206	55	89	
B19	164	#4	205	59	97	96
B19	172	#4	218	47	100	
B19	184	#4	221	60	96	
B1	175	#4	185	53	90	
B2	167	#4	156	46	100	
B20	267	#6	206	68	86	54
B13	143	#4	170	47	67	
B15	174	#4	159	48	64	
B3	183	#4	162	63	22	
B22	160	#4 TDL?				38
B22	175	#4	137	60	40	53
B22	195	Control				5
B25	5	Control				9
B25	210	Control				10

Summarized sand and marine tracer analyses are presented for correlated inundation events (#) recorded in core sites (Figures 9, 12, and 14) from the Neskowin and Beaver localities. Mean grain size (Mean G.S.) and standard deviation of grain size (±1σ SD) of the sand size fraction are in micrometers (μm).

Normalized heavy-mineral rounding (Mineral % Marine) yields percentage marine sand relative to alluvial sand supply as based on end-member (beach and creek) sand compositions.

Marine diatom taxa (Diatom % Marine) are based on whole frustual counts of marine, brackish, and freshwater taxa (Schlichting, 2000). Data are shown as percent, but fewer than 100 whole diatom frustules were observed in most samples. See Appendix ([insert url for online-only datasets here]) for detailed grain size, mineral rounding. and diatom taxa data.

sample heavy-mineral fractions (density >2.9 g cm^{-3}) under a petrographic microscope at 250×. Percentage beach sand component is based on normalized ratios of the rounded (marine) and angular (river) augite grains from end-member beach and creek samples, respectively (Table 3). Though not presented here, the creek and beach sands in north-central Oregon are also differentiated by the augite to hypersthene ratio, with hypersethene largely restricted to the beach sand source (Schiedegger, Kulm, and Runge, 1971).

The paleotsunami sand layers from events #2 and #3 in the Hawk flood plain sites of Neskowin show large components of marine sand (76%–87%) in the heavy mineral fraction (Table 3). We do not differentiate inner-shelf, beach, and dune sources of the marine sand component in this study. The high percentages of beach sand component in the Hawk flood plain

Figure 11. Photograph of event #3 paleotsunami sand layer (TSL at 185–186 cm depth) and overlying tsunami debris layer (TDL at 180–185 cm depth) in site B3. Note: Add 100 cm to 1-m field tape scale measured sand size of basal tsunami sand layer is 162 ± 63 μm (Table 3).

Figure 12. Photograph of #3 paleotsunami debris layer (TDL at 171–179 cm depth) in site B4. Note: Add 100 cm to the 1-m field tape scale. The tsunam debris layer grades upward from fine sand disseminated in silt (179–177 cm depth) to fine sand disseminated in coarse detrital organics (177–171 cm depth).

sites show relatively little recharging of the paleotsunami surge(s) from creek or flood plain sand. The dominant beach sand component suggests an inundation of the Hawk flood plain by direct paleotsunami overtopping of the Neskowin barrier ridges (Figure 5), rather than by backwash flooding from the Neskowin Creek to the south.

Sand source indicators of tsunami flooding in Beaver valley are variable over the several kilometer distance of inundation. The beach sand component of the heavy-mineral fraction in event #3 sand layers decreases from the proximal site B19 (~95%) to the most distal site B3 (22%) (Table 3). Generally, the more proximal sites (1–2 km inland distance) retained very-high components of beach sand (90%–100%), but sand recharging from alluvial sources diluted the beach sand component in more distal sites (3–4 km distance). High abundances of beach sand also confirm paleotsunami origins for the younger sand layers at 52 and 88 cm depth in site B19, and the older sand layer at 267 cm depth in site B20.

Whole diatom frustules, including 10 marine taxa, 22 brackish taxa, and 15 freshwater taxa, were identified from selected paleotsunami deposits and control intervals in the Neskowin and Beaver flood plains. The percentage of marine taxa has been used as a proxy for paleotsunami inundation in the freshwater back-barrier wetlands of northern Oregon and southern Washington (Schlichting, 2000). The results of the diatom analyses from Neskowin and Beaver core samples are summarized in Table 3.

The paleotsunami layers (#2 and #3) in the Hawk flood plain of Neskowin yield ~50%–100% marine diatoms (Table 3). Control intervals (nontsunami intervals) ranged from ~0% to 20% marine taxa. The presence of some marine taxa in most control intervals indicates transport of marine diatoms into the flood plain, likely by wind-swept ocean spray. In Beaver valley, the #3 paleotsunami layer ranged from ~40% to 95% marine diatoms. Control intervals from the north Beaver valley yielded 5%–10% marine diatoms. An extended record of marine diatoms (~40% marine taxa) occurs at 15 cm above the event #3 sand layer at site B22 (Figure 10b). This 15 cm thick interval demonstrates the prolonged impact of catastrophic tsunami inundation on the microfossil record in bioturbated deposits of the flood plain.

Although diatoms help to confirm marine surge origins for the selected sand layers in the Neksowin and Beaver flood plains (Table 3), they are considered less reliable than the marine sand tracers in the study area. The total diatom counts in some Neskowin and Beaver flood plain deposits (15–25 diatoms per 1–3 g of sediment) are 1%–10% of the expected diatom abundances, as typically found in pallustrine marsh and pond settings in the field area (Schlichting, 2000). The low diatom abundances make these flood plain settings susceptible to bias from apparent wind transported marine diatoms (~5%–20%), as found in some nonpaleotsunami intervals. Caution is warranted in relying on marine diatoms as the sole indicator of paleotsunami inundation in distal flood plain settings of wind-swept coastlines.

DISCUSSION

Event Correlation

Several steps are employed to tie the Neskowin and Beaver marine inundations to established records of Cascadia near-field paleotsunami. Reported rupture subsidence and corresponding paleotsunami deposits are correlated in small estuaries within the study area, Siletz, Yaquina, and Alsea bays (Figure 2). Five paleotsunami events during the last

Table 4. *Regional correlation of overland inundations from nearfield paleotsunami during the last ~2500 years in the Cascadia margin.*

Localities	TSL #1 Rupture Y 0.3 ka	TSL #3 Rupture W ~1.1 ka	TSL #4 Rupture U ~1.3 ka	TSL #5 Rupture S ~1.7 ka	TSL #6 Rupture N ~2.6 ka
Kanim*					2650–2800
Deserted*	360–570		1580–1870		2450–2900
Long Beach	×	×	920–1285		
Seaside			1060–1260		2780–2950
Cannon	×	×	1276–1411		
Neskowin		×	1140–1300		
Beaver	320–520		1520–1700		2960–3220
Lagoon*	270–560	970–1290	1270–1520	1290–1710	2340–2760

Dated overland inundations leaving tsunami sand layers (TSL) from nearfield events #1, #3, #4, #5, and #6 in localities from the Cascadia margin (Figure 1). Corresponding Cascadia ruptures (letter codes Y, W, U, S, and N) and estimated rupture dates (in ka) are from Atwater *et al.* (2004).

Key paleotsuunami deposit dates are shown in 2σ calibrated radiocarbon YBP for correlation purposes.

Overland run-ups from nearfield paleotsunami are shown (x) for Long Beach (Schlichting, 2000), Seaside (Peterson *et al.,* unpublished data), Cannon Beach (Peterson *et al.,* 2008), and Neskowin and Beaver (this article). The largest inundations in the central Cascadia localities are shown with event deposit dates.

The thresholds for largest overland run-ups in the central Cascadia margin are (1) ~1.0 km inundation distance in Long Beach, (2) >8 m elevation NAVD88 proximal run-up height in Seaside, (3) >1.5 km inundation distance in Cannon Beach, (4) >8 m elevation NAVD88 distal run-up height in Neskowin, and (5) >1.5 km inundation distance in Beaver.

* All reported events from the last ~2500 years are shown for Kanim Lake (Hutchinson, Clague, and Mathewes, 1997), Deserted Lake (Hutchinson *et al.,* 2000), and Lagoon Creek (Abramson, 1998).

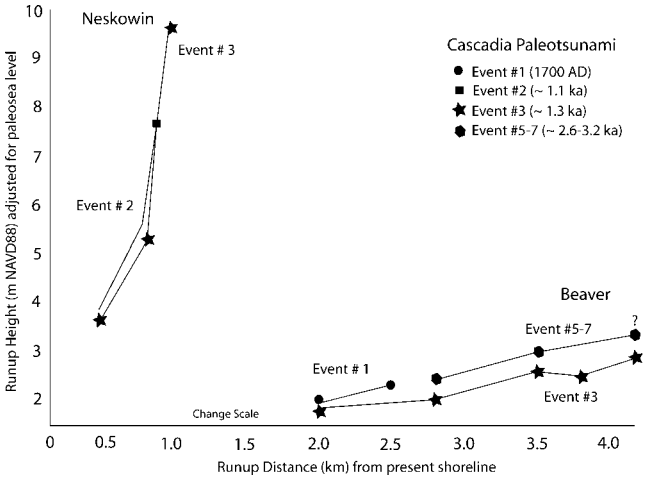

Figure 13. Run-up distance (km) and height (m) of paleotsunami deposits (lines) from events #2 and #3 in Neskowin and events #1, #3 and #5–7 in Beaver. Recorded run-ups at key core sites are shown by bold symbols for corresponding large paleotsunami inundations. The terminal deposit for event #5–7 at Beaver is tentative. See [insert url for online-only datasets here] for details of core site elevations, deposit depths, and paleosea level adjustments (1 m/1000 y relative sea level rise) corresponding to the correlated Cascadia paleotsunami events. See Supporting Materials (see details at [insert url for online-only datasets here]) for details of core site elevations, deposit depths, and paleosea level adjustments (1 m/1000 y relative sea level rise) corresponding to the correlated Cascadia paleotsunami events.

~2600 years are correlated between the small estuaries and well-established megathust ruptures recorded by coseismic subsidence in southwest Washington (Atwater *et al.,* 2004) (Table 1). Three particularly robust inundations occurred in the central Oregon bays, including events #1 (1700 AD), #3 (~1.3 ka) and #5 (~2.6 ka).

Published records of overland paleotsunami run-up are compiled from back-barrier wetland settings at Long Beach, Washington, and Seaside and Cannon Beach, Oregon (Table 4). Overland inundation from nearfield paleotsunami events #1, #2, #3, and #5/6 are recorded in these back-barrier settings. The largest paleotsunami run-ups, based on inundation distance and/or relative run-up height, were produced by events #3 and #5/6. These two events apparently yielded the longest inundation records in Beaver valley (Figures 10a and b). The #3 event produced the highest sand-sheet deposits in the Hawk Creek flood plain of Neskowin (Figures 5 and 7).

Large paleotsunami events in the study area are compared with overland paleotsunami records in northern Cascadia (Kanim and Deserted Lakes) and in southern Cascadia (Lagoon Creek) (Figure 1). The northern Cascadia localities record events #1, #3, and #5 (Table 4) (Hutchinson, Clague, and Mathewes, 1997; Hutchinson, *et al.,* 2000). Lagoon Creek in the southern Cascadia margin records events #1, #2, #3, #4, and #5, with event #1 yielding the weakest sand layer record (Abramson, 1998). There is one additional sand layer (#6) from a single proximal core site in Lagoon Creek with a reported age of 3060–3470 cal YBP.

The largest run-up record preserved in both Neskowin and Beaver, paleotsunami #3 (~1.3 ka), is correlated to overland run-up records from the full length of the Cascadia margin (Table 4, Figure 1). The second highest paleotsunami run-up in Neskowin from event #2 (~1.1 ka) is correlated to overland run-up in Lagoon Creek in the southernmost Cascadia margin. The paleotsunami with the third longest run-up in Beaver, event #1 (1700 AD), is correlated to run-up in Deserted Lake, but not in Kanim Lake, in the northern Cascadia margin and to weak overland run-up in Lagoon Creek in the southern Cascadia margin.

Maximum Recorded Paleotsunami Run-up

The field studies in Neskowin and Beaver were undertaken to verify the suitability of flood plains in hosting and preserving distal records of the larger paleotsunami inundations. A trial of this approach was conducted in the Ecola Creek flood plain in Cannon Beach, Oregon (Peterson, Cruikshank, and Schlichting, 2008). The results from that study yielded a maximum run-up of ~6 m, at a distance of 1.5–2.0 km from the beach for the central Cascadia #3 paleotsunami (Table 4).

That same #3 paleotsunami (~1.3 ka) provides the greatest run-up recorded during the last 1500 years at both Neskowin and Beaver (see details at [insert url for online-only datasets here]). The maximum-recorded run-up, based on sand sheet extent, reached at least 8.3 m elevation in Hawk Creek, Neskowin. Adjusting for a lower paleo–sea level at 1.3 ka (~1 m/1000 y relative sea level rise), we estimate a distal run-up of at least 9 m at a distance of ~1 km for the #3 paleotsunami surge(s) at Neskowin (Figure 13). In the lower gradient flood

plain of Beaver valley (elevation 3 m) the #3 paleotsunami event inundated to an up-valley distance of at least 4.1 km. A significant widening of the North Beaver valley at ~3 km (Figure 9) might have attenuated the overland flow, resulting in a transition from sand sheet deposition to detrital layer deposition at ~3.5 km distance.

Three other paleotsunami events are recorded in the distal flood plain localities of Neskowin and Beaver valley (Figure 13). A terminal inundation from event #2 at ~1.1 ka (Table 2) left a rarely preserved debris layer in the Hawk Creek flood plain. The deepest paleotsunami sand sheet observed in Beaver (event #5–7) might equal the inundation distance of the younger inundation from event #3. A modest terminal inundation from paleotsunami event #1 (1700 AD) reached 2.0 km in Beaver Valley (2–3 m elevation), but it lacked sufficient amplitude to leave a preserved record in the Hawk Creek flood plain at Neskowin. The combinations of thinning paleotsunami deposits together with seasonal oxidation and bioturbation of hosting soils in the distal flood plain settings limit the preserved record of maximum inundation. Nevertheless, the flood plain settings permit a doubling or tripling of recorded inundation distance from back-barrier wetlands in both the Neskowin and Beaver localities. The use of flood plain settings should substantially extend the geologic records of paleotsunami or storm surge inundation in other coastlines that experience these hazards.

CONCLUSIONS

In this study of overland paleotsunami run-up, we examine two localities, Neskowin and Beaver, Oregon, with alluvial flood plains that extend well landward of their back-barrier wetlands. The two localities host the highest and longest records of distal overland run-up reported to date for the coseismic Cascadia margin. The two largest paleotsunami are correlated to a regionally recorded Cascadia paleotsunami at ~1.3 ka, and to an older event (between 2.6 and 3.2 ka). Two smaller nearfield paleotsunami, correlated to Cascadia events at ~1.1 ka and 1700 AD, are also recorded in the Neskowin and Beaver flood plains, respectively. The flood plain settings present difficulties of paleotsunami record preservation, including channel avulsion, wind transported marine diatoms, and extensive bioturbation of the flood plain deposits. However, locally preserved stratigraphic records in flood plain deposits do permit the tracing of the larger paleotsunami inundations to positions well landward of back-barrier wetlands. Undisturbed flood plain deposits potentially extend the landward record of catastrophic inundation, yielding better estimates of surge run-up in susceptible coastlines.

ACKNOWLEDGMENTS

This study was completed in several parts. Tim Barnes, Michael Boynay, Thomas Braibish, Douglas Hanson, Paul Glenn, Taryn Eddy, and Sheryl Zinsli assisted with reconnaissance searches for paleotsunami inundation records in the Neskowin area barrage ponds (Daley Lakes) in 1994. Frank Cranshaw, Nichole Alhadeff, Darren Beckstrand, Torin Emerson, Glen Gettemy, Gloria Holthaus, Andrew Manning, Torrey Nyborg, Chandra Robinson, and Mike Vedder assisted with reconnaissance coring in the back-barrier wetlands of Beaver Creek in 1998. Anna Pilette, Brandon Ezzell, Mathew Brown, Adam Cambell, Aspen Gillam, Joshua Hackett, Rachel Piort, and Joshua Theule assisted with reconnaissance coring in the upper Beaver Creek Valley in 2007. Funding for the paleotsunami inundation mapping in the back-barrier wetlands of Neskowin and Beaver Creek valley was provided the National Oceanic and Atmospheric Administration Office of Sea Grant and Extramural Programs under grant NA36RG0451, project R/CP-28 and by the Office of Sponsored Research at Portland State University.

LITERATURE CITED

Abramson, H.F., 1998. Evidence for Tsunamis and Earthquakes during the Last 3500 years from Lagoon Creek. A Coastal Freshwater Marsh, Northern California. Arcata, California: Humboldt State University, Master's thesis, 76p.

Alhadeff, N.; Beckstrand, D.; Emerson, T.; Gettemy, G.; Holthaus, G.; Manning, A.; Nyborg, T.; Robinson, C., and Vedder, M., 1998. Preliminary Survey of Paleotsunami Deposits at Ona Beach, Oregon. Portland, Oregon: Oregon Department of Geology and Mineral Industries, 14p.

Atwater, B.F., 1987, Evidence for great Holocene earthquakes along the outer coast of Washington State. *Science,* 336, 942–944.

Atwater, B.F.; Nelson, A.R.; Clague, J.L.; Carver, G.A.; Yamagouchi, D.K.; Bobrowsky, P.T.; Bourgeois, J.; Darienzo, M.E.; Grant, W.C.; Hemphill-Haley, E.; Kelsey, H.M.; Jacoby, G.C.; Nishenko, S.P.; Palmer, S.P.; Peterson, C.D., and Reinhart, M.A., 1995. Summary of coastal geologic evidence for past great earthquakes at the Cascadia Subduction Zone. *Earthquake Spectra,* 11, 1–18.

Atwater, B.F.; Tuttle, M.P.; Schweig, E.S.; Rubin, C.M.; Yamaguchi, D.K.; and Hemphill-Haley, E., 2004. Earthquake recurrence, inferred from paleoseismology. *In:* Gillespie, A.R., Porter, S.C., and Atwater, B.F. (eds.), *The Quaternary Period in the United States.* Amsterdam: Elsevier, pp. 331–350.

Boynay, M.A.; Barnes, T.; Berry, J.; Braibish, T.; Clark, L.; Eddy, T.; Glenn, P.; Groseclose, M.; Hanson, D.; Heupel, N.; Kalli, G.; Kickman, S.; Peterson, C.D.; Ree T.; Rosenberger, D.; Rosenberger, K.; Sheldon-Wambaugh, C.; Stack, C., and Zinsli, S., 1994. Paleotsunami Records in Daley Lake, Dune Barrage Lake, Central Coast of Oregon. Camp Winema, Oregon: Camp Winema Directors, 25p.

Clague J.J. and Bobrowsky P.Y., 1994. Tsunami deposits beneath tidal marshes on Vancouver Island, British Columbia. *Geological Society of America Bulletin,* 106, 1293–1303.

Clemens, K.E. and Komar, P.D., 1988. Oregon beach sand compositions produced by mixing of sediments under a transgressing sea. *Journal of Sedimentary Petrology,* 58, 519–529.

Cruikshank, K.M., and Peterson, C.D., 2008. Oregon_Tsunami_Database. Electronic Access Database File and Report. http://geomechanics.geol.pdx.edu/Projects/Tsunami (accessed May 15, 2008).

Darienzo, M.E., 1991. Late Holocene Paleoseismicity along the Northern Oregon Coast. Portland, Oregon: Portland State University, Ph.D. thesis, 167p.

Darienzo, M.E.; Craig, S.; Peterson, C.D.; Watkins, A.; Winke, D.; Wieting, A., and Doyle, A., 1993. Extent of Tsunami Sand Deposits Landward of the Seaside Spit. Clatsop County, Oregon: Clatsop County Sheriffs, 21p.

Darienzo, M.E. and C.D. Peterson, 1990. Episodic tectonic subsidence of late-Holocene salt marsh sequences in Netarts Bay, Oregon, Central Cascadia Margin, USA. *Tectonics,* 9, 1–22.

Darienzo, M.E.; Peterson, C.D., and Clough, C., 1994, Stratigraphic evidence for great subduction zone earthquakes at four estuaries in northern Oregon, *Journal of Coastal Research,* 10, 850–876.

Dawson, A.G. and Shi, S.Z., 2000. Tsunami deposits. *Pure and Applied Geophysics,* 157, 875–897.

Fiedorowicz, B.K., 1997. Geologic Evidence of Historic and Prehis-

toric Tsunami Inundation at Seaside, Oregon. Portland, Oregon: Portland State University, Master's thesis, 197p.
Garrison-Laney, C.E., 1998. Diatom Evidence for Tsunami Inundation from Lagoon Creek, a Coastal Freshwater Pond, Del Norte County, California. Arcata, California: Humboldt State University, Master's thesis, 97p.
Hutchinson, I.; Clague, J.J., and Mathewes, R.W., 1997. Reconstructing the tsunami record on an emerging coast: a case study of Kanim Lake, Vancouver Island, British Columbia, Canada. *Journal of Coastal Research,* 13, 545–553.
Hutchinson, I.; Guilbault, J.P.; Clague, J.J., and Bobrowsky, P.T., 2000. Tsunamis and tectonic deformation at the northern Cascadia margin: a 3,000 year record from Deserted Lake, Vancouver Island, British Columbia, Canada. *The Holocene,* 10, 429–439.
Kelsey, H.M.; Nelson, A.R.; Hemphill-Haley, E., and Witter, R.C., 2005, Tsunami history of an Oregon coastal lake reveals a 4600 yr record of great earthquakes on the Cascadia subduction zone. *Geological Society of America, Bulletin,* 117, 1009–1032.
Peterson, C.D.; Chadha, R.K.; Cruikshank, K.M.; Francis, M.; Latha, G.; Katada, T.; Singh, J.P., and Yeh, H., 2006. Preliminary comparison of December 26, 2004 tsunami records from SE India and SW Thailand to paleotsunami records of overtopping height and inundation distance from the central Cascadia margin, USA. *In: NCEE 8th Annual Proceedings,* Paper 8NCEE-001859 on CD-ROM.
Peterson, C.D.; Cruikshank, K.M.; Jol, H.M., and Schlichting, R.B., 2008. Minimum runup heights of paleotsunami from evidence of sand ridge overtopping at Cannon Beach, Oregon, Central Cascadia Margin, USA. *Journal of Sedimentary Research,* 78, 390–409.
Peterson, C.D. and Darienzo, M.E., 1997. Discrimination of flood, storm and tectonic subsidence events in coastal marsh records of Alsea Bay, Central Cascadia Margin, USA. *In:* Rogers, A.M., Walsh, T.J., Kockelman, W.J., and Priest, G.R. (eds.), *Assessing and Reducing Earthquake Hazards in the Pacific Northwest,* Volume 1, pp. 115–146, USGS Professional Paper 1560. Washington, D.C.: U.S. Geological Survey.
Peterson, C.D.; Darienzo, M.E.; Doyle, D., and Barnett, E., 1996. Evidence for coseismic subsidence and tsunami inundation during the past 3000 years at Siletz Bay, Oregon. *In:* Priest, G.R. (ed.), Open-File Report O-95-05. Portland, Oregon: Oregon Department of Geology and Mineral Industries, pp. 45–69.
Peterson, C.D.; Darienzo, M.E.; Hamilton, D.; Pettit, D.J.; Yeager, R.K.; Jackson, P.L.; Rosenfeld, C.L., and Terich, T.A., 1994. Cascadia Beach-Shoreline Data Base, Pacific Northwest Region, USA. Oregon Department of Geology and Mineral Industries Open-File Report 0-94-2, 29p., and 3 electronic database files.
Peterson, C.D.; Doyle, D.L., and Barnett, E.T., 2000. Coastal flooding and beach retreat from coseismic subsidence in the central Cascadia margin, USA. *Environmental and Engineering Geology,* 6, 255–269.
Peterson, C.D. and Priest, G.R., 1995. Preliminary reconnaissance survey of Cascadia paleotsunami deposits in Yaquina Bay, Oregon. *Oregon Geology,* 57, 33–40.
Peterson, C.D.; Scheidegger, K.F., and Komar, P.D., 1982. Sand dispersal patterns in an active- margin estuary of the northwestern United States as indicated by sand composition, texture and bedforms. *Marine Geology,* 50, 77–95.
Reimer, P.J.; Baillie, M.G.L.; Bard, E.; Bayliss, A.; Beck, J.W.; Bertrand, C.; Blackwell, P.G.; Buck, C.E.; Burr, G.; Cutler, K.B.; Damon, P.E.; Edwards, R.L.; Fairbanks, R.G.; Friedrich, M.; Guilderson, T.P.; Hughen, K.A.; Kromer, B.; McCormac, F.G.; Manning, S.; Bronk Ramsey, C.; Reimer, R.W.; Remmele, S.; Southon, J.R.; Stuiver, M.; Talamo, S.; Taylor, F.W.; van der Plicht, and Weyhenmeyer, C.E., 2004. *Radiocarbon,* 46, 1029–1058.
Satake, K.; Shimazaki, K.; Tsuji, Y., and Ueda, K., 1996, Time and size of giant earthquake in Cascadia inferred from Japanese tsunami records of January 1700. *Nature,* 378, 246–249.
Schiedegger, K.F.; Kulm, L.D., and Runge, E. J., 1971. Sediment sources and dispersal patterns of Oregon continental shelf sands. *Journal of Sedimentary Petrology,* 41, 1112–1120.
Schlichting, R.B., 2000. Establishing the Inundation Distance and Overtopping Height of Paleotsunami from Late-Holocene Geologic Records at Open-Coastal Wetland Sites, Central Cascadia Margin. Portland, Oregon: Portland State University, Master's thesis, 166p.
Schlichting, R.B. and Peterson, C.D., 2006. Mapped overland distance of paleotsuami high-velocity inundation in back-barrier wetlands of the Central Cascadia Margin, USA. *Journal of Geology,* 114, 577–592.
Shennan, I.; Long, A.J.; Rutherford, M.M.; Innes, J.B.; Green, F.M., and Walker, K.J., 1998. Tidal marsh stratigraphy, sea-level change and large earthquakes: submergence events during the last 3500 years at Netarts Bay, Oregon, USA. *Quaternary Science Reviews,* 17, 365–393.
Shiki, T.; Tachibana, T.; Fujiwara, O.; Goto, K.; Nanayama, F., and Yamazaki, T., 2008. Characteristic features of tsunamiites. *In:* Shiki,T., Minoura, K., Tsuji, Y., and Yamazaki, T. (eds.), *Tsunamiites–Features and Implications,* Chapter 1. Amsterdam: Elsevier, pp. 319–340.
U.S. Geological Survey Water Resources, 2007. Surface Water Data for Oregon. USGS Surface-Water Annual Statistics. http://waterdata.usgs.gov/or/nwis/annual/ (accessed May 1, 2008).
U.S. Geological Survey, 2008. Seamless Map Data. http://seamless.usgs.gov/. (accessed June 28, 2007).